NANO LETTERS

2002
Vol. 2, No. 9
941−944

Helical Crystalline SiC/SiO_2 Core–Shell Nanowires

Hai-Feng Zhang,[†,‡] Chong-Min Wang,[‡] and Lai-Sheng Wang*[,†,‡]

Department of Physics, Washington State University, 2710 University Drive, Richland, Washington 99352, and W. R. Wiley Environmental Molecular Sciences Laboratory, Pacific Northwest National Laboratory, P.O. Box 999, Richland, Washington 99352

Received June 25, 2002

ABSTRACT

Helical crystalline silicon carbide nanowires covered with a silicon oxide sheath (SiC/SiO_2) have been synthesized by a chemical vapor deposition technique. The SiC core typically has diameters of 10–40 nm with a helical periodicity of 40–80 nm and is covered by a uniform layer of 30–60 nm thick amorphous SiO_2. A screw-dislocation-driven growth process is proposed for the formation of this novel structure based on detailed structural characterizations. The helical nanostructures may find applications as building blocks in nanomechanical or nanoelectronic devices. The screw-dislocation-induced growth mechanism suggests that similar helical nanostructures of a wide range of materials may be synthesized.

One-dimensional (1D) nanostructures have potential applications as interconnects or functional components in nanoscale electronic, optoelectronic, or mechanical devices.[1,2] A variety of 1D systems have been synthesized, including carbon nanotubes,[3] semiconductor nanowires,[4−9] coaxial nanocables,[10] and nanobelts.[11,12] Although helical nanostructures are common in biology[13,14] and self-assembled organic systems,[15,16] similar nanostructures are difficult to realize in inorganic materials.[17−19] Here we report the synthesis of helical crystalline silicon carbide nanowires covered with a silicon oxide sheath. Large quantities of the helical SiC/SiO_2 core−shell structures tens of micrometers long were synthesized by a chemical vapor deposition technique. The SiC core typically has diameters of 10−40 nm with a helical periodicity of 40−80 nm and is covered by a uniform layer of 30−60 nm thick amorphous SiO_2. Detailed structural characterizations suggested that the growth of this novel structure was induced by screw dislocations on the nanometer scale.

The composite helical silicon carbide nanowires were synthesized in a flow-tube furnace using iron-catalyzed decomposition of methane at 1100 °C. Iron powders[20] were held in an alumina sample boat upstream in the flow tube and a silicon wafer located down stream was used as the substrate. A reaction time of 5−10 min plus a 1-h postreaction treatment under the same high-temperature conditions were sufficient to grow a large quantity of nanostructures on the silicon wafer. The as-synthesized sample on the silicon substrate was observed as a fluffy material. Scanning electron microscope (SEM) revealed that most of the materials are wire-like structures with diameters in the nanometer size range and tens of micrometers long, as shown in Figure 1.

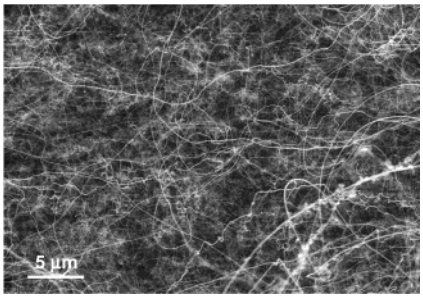

Figure 1. SEM characterization of as-synthesized silicon carbide nanowires. A LEO DSM 982 Gemini digital field emission scanning electron microscope was used. The synthesis was performed in a horizontal alumina tube furnace using a silicon wafer as substrate, which was scratched using a 600 grit sand paper. Iron powders, held in an alumina sample boat and used as a catalyst to decompose methane, were placed in the tube furnace upstream from the silicon substrate. The synthesis is carried out as follows. (1) Increase the temperature slowly to 1100 °C with a 200 cm^3/min argon flow and hold at this temperature for 30 min (preheating). (2) Switch on methane flow at 40 cm^3/min and maintain a 160 cm^3/min argon flow for 5 to 10 min. (3) Turn off the methane flow and keep the argon flow at 1100 °C for 1 h (postreaction heat treatment). The as-synthesized materials consist mainly of nanowires with uniform diameters and up to several hundred micrometers long.

Low magnification transmission electron microscopy (TEM) showed that there were straight and curled wire-like structures, all with uniform diameters (Figure 2a). With increasing magnification, we were surprised to observe that a large number of the nanowires are in fact of helical shape with a clear core−shell structure (Figure 2b,c). Using high-resolution TEM (HRTEM), electron diffraction, and elemen-

* Corresponding author. E-mail: ls.wang@pnl.gov.
† Washington State University.
‡ W. R. Wiley Environmental Molecular Sciences Laboratory.

10.1021/nl025667t CCC: $22.00
Published on Web 07/26/2002

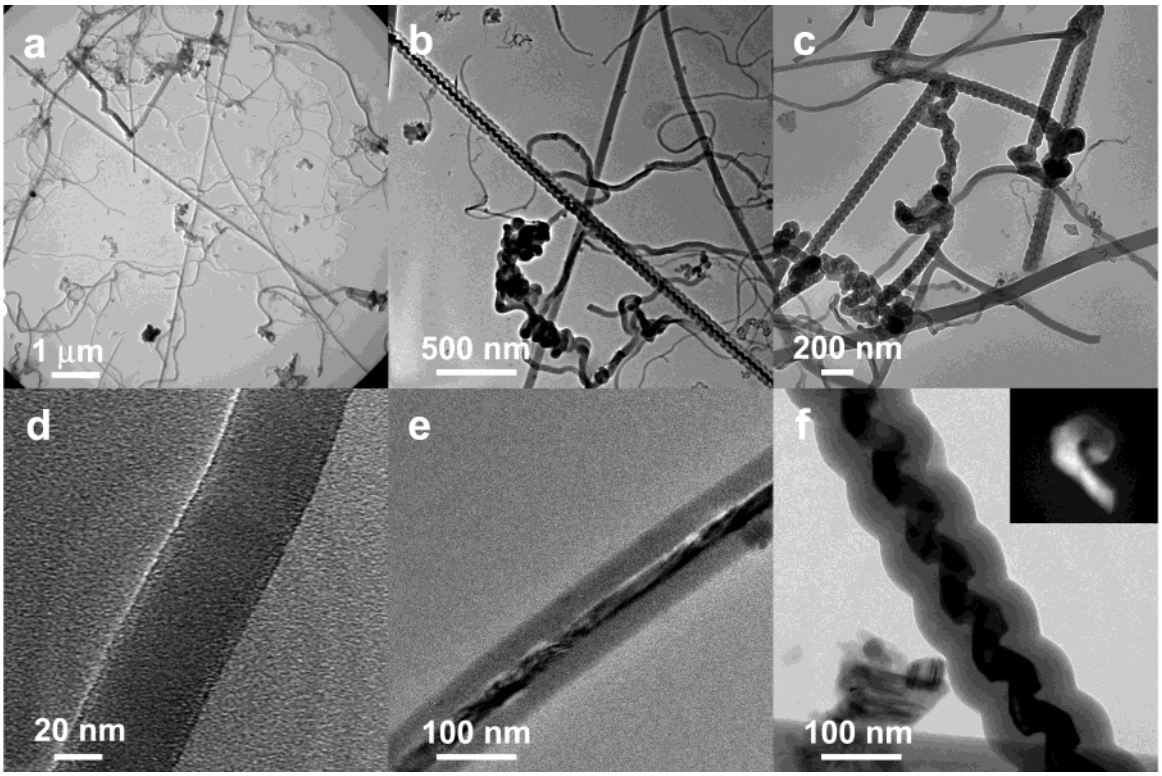

Figure 2. TEM characterization of nanowires. (a) Low magnification TEM image showing a variety of nanowires. (b) TEM image showing a long helical SiC/SiO_2 core−shell nanostructure. (c) A selected area with a high density of helical core−shell wires. (d) HRTEM image of an amorphous SiO_2 nanowire. (e) HRTEM image of a straight SiC nanowire with an amorphous SiO_2 sheath. (f) HRTEM image of a helical SiC nanowire with an amorphous SiO_2 sheath. The inset shows a dark field TEM image of a helical nanowire taken along the helical axis (wire diameter, ~22 nm). The TEM characterization was performed with a JEOL JEM-2010 instrument operated at 200 keV. Samples were transferred from the silicon substrate to a carbon-coated Cu grid TEM sample holder using a solution method: the silicon substrate was dipped into 10 mL ethanol and ultrasonicated for 1 min; then several drops of the ethanol solution were put onto the TEM grid.

tal analyses, we found that there are three types of nanowires, (1) pure amorphous SiO_2 (Figure 2d), (2) linear β-SiC/SiO_2 core−shell nanowires (Figure 2e), and (3) helical β-SiC/SiO_2 core−shell nanowires (Figure 2f). The inset of Figure 2f is a cross-section-like dark field TEM image of the helical structure taken along the helical axis. It shows clearly that the shape of the helical structure is not cylindrical, but rather hexagonal-like, which suggests that the helical axis is along the β-SiC [111] direction. The overall diameters of the three types of nanostructures were similar with about the same size distributions and almost equal amount in the as-synthesized samples. Amorphous SiO_2 and linear β-SiC/SiO_2 nanowires were synthesized previously,[21−24] but the helical β-SiC/SiO_2 nanowires have never been seen before.

HRTEM images, FFT-filtered lattice image, and electron diffraction (Figure 3) confirmed that the helical core is well-ordered β-SiC with diameters ranging from 10 to 40 nm. High densities of planar defects were observed, which were also common in the straight SiC nanowires.[23,24] Chemical mapping for oxygen (Figure 3b) clearly indicated that the helical core is oxygen deficient, consistent with the HRTEM and diffraction analyses. The amorphous SiO_2 layer always has uniform thickness, ranging from 30 to 60 nm and yielding an overall helical shape for the core−shell composite nanostructures (Figures 2 and 3) very similar to a typical coiled telephone cord. All the helical nanowires have uniform periodicity between 40 and 80 nm, depending on the diameter of the SiC core. The cross section of the SiC core was not definitely known. The contrast and clear edge in the HRTEM images (Figure 3a, c) suggest that the β-SiC core may be square/rectangular instead of cylindrical.

Figure 4a displays a TEM image of a helical nanowire attached to a nanoparticle inside an amorphous SiO_2 layer. Figure 4b is a dark TEM image, showing that the nanoparticle is a crystalline material. This nanoparticle may be critical for the formation of the helical nanowires, either as catalysts or the initial nucleation sites. High-resolution TEM imaging (Figure 4c) and FFT-filtered lattice images (insets of Figure 4c) revealed that the nanoparticle and the adjacent helical nanowire are both made of crystalline SiC. Energy-dispersive X-ray (EDX) analyses (Figure 4d) revealed that the nanoparticles with the amorphous shell are composed of Si, C, O, and a small amount of Al (the Cu signal was from the carbon-covered copper TEM grid, which also contributed to the C signal). The nanoparticles found at the end of the helical nanowires are different from the catalytic particles, typically found at the tip of the straight SiC nanowires, which are mainly composed of Fe and a small amount of C and Si. The morphologies of the nanoparticles are also different: the Fe-dominated nanoparticles found on the straight nanowires are usually spherical while the nanoparticles found on the helical nanowires are usually faceted. These differences in

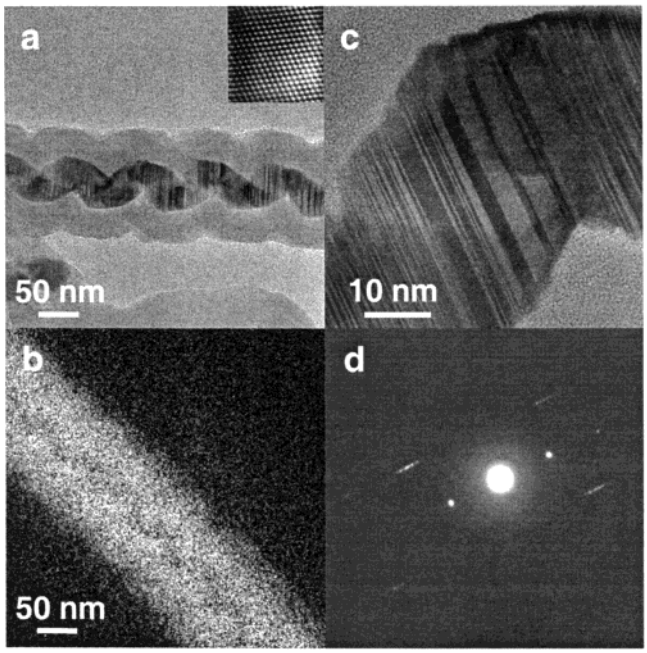

Figure 3. TEM characterization of helical SiC nanowires. (a) HRTEM image of a section of a helical SiC nanowire. The inset is an FFT filtered lattice image of a part of the helical SiC nanowire in (c), showing that the SiC core is highly crystalline. (b) Chemical mapping for oxygen calculated by the three-window method using preedge and postedge images at the oxygen-K edge. (c) HRTEM image of a portion of a helical SiC nanowire. (d) A diffraction pattern from a spot on the helical nanowire in (c). Both the inset in (a) and the diffraction pattern in (d) confirm the crystalline material is β-SiC.

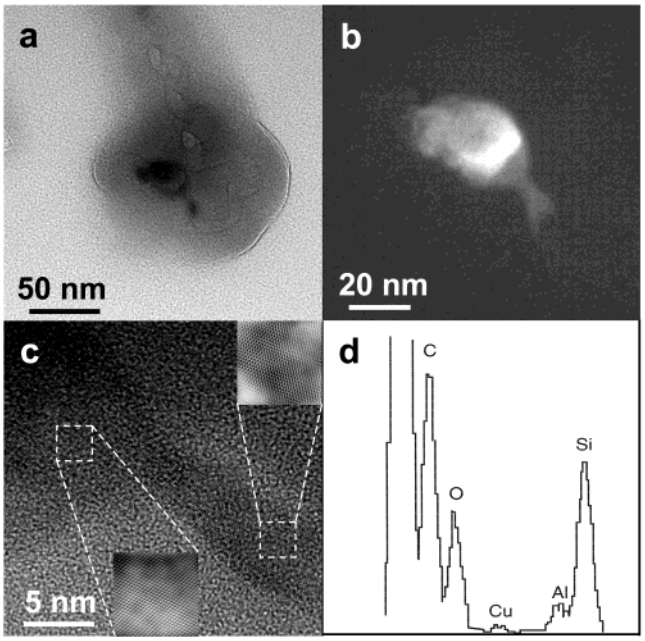

Figure 4. (a) Bright field TEM image of a helical nanowire with a nanoparticle attached at its tip. (b) Dark field TEM image of the nanoparticle in (a), showing in more detail the interface between the nanoparticle and the helical nanostructure. (c) HRTEM image of the interface part between the helical structure and nanoparticle. The insets are the FFT-filtered lattice images of two separated areas in (c), showing that both the nanoparticle and the growing helical structure are β-SiC. (d) EDX of the nanoparticle including the amorphous shell in (a).

the nanoparticle shapes and compositions may indicate that the formation mechanisms of the helical and straight nanowires are different.

The formation of straight SiC nanowires is catalyzed by the Fe nanoparticles and can be described by the V−L−S growth mechanism.[1] For catalytically grown helical carbon nanotubes, Amelinckx et al.[25] proposed a formation mechanism by introducing the concept of spatial velocity hodograph, suggesting that the driving force was due to both the changing deposition rates along a circle of growth front and a local motion of the catalytic particles. Suenaga et al. observed coiled nanostructures of eccentric coaxial nanocable made of amorphous boron with a SiO_2 sheath,[26] and they attributed the formation of the coiled structure to a difference in the growth rates between the core amorphous boron and the SiO_2 outer layer. Other models based on growth anisotropies have been proposed very recently to explain the formation of amorphous BC and pure C nanocoils.[18,19] Our HRTEM images showed that the crystalline β-SiC core in our helical nanowires is always in the center of the coaxial core−shell assembly. There must be a different growth mechanism for the formation of this 1D helical nanostructure.

The helical SiC/SiO_2 nanowires were primarily grown during the postreaction heat treatment, during which C and SiO probably reacted on the crystalline SiC nanoparticles to form the SiC/SiO_2 composite nanowires in the following stoichiometry: $2SiO + C \rightarrow SiC + SiO_2$. The carbon source was from the Fe-catalyzed CH_4 decomposition in the initial methane flow,[27] and the SiO source was from the surface of the silicon substrate. While the driving forces for the formation of helical structures in biological and organic systems are H-bonding and other noncovalent interactions,[13−16] what is the driving force for the formation of the helical SiC nanowires? On the basis of our structural analyses, here we propose a growth mechanism that derives from screw dislocations present in the initial crystalline SiC nanoparticles, as shown in Figure 5. The diameters of the SiC cores are determined by the size distribution of the initial nucleation sites. The SiO_2 outer layer grown simultaneously may play an important role in stabilizing the helical SiC nanowire core.

Figure 5a,b shows the schematic drawings of two blocks of materials, each containing a screw dislocation with Burgers vector, u,[28] and helical ramps (helical lattice "planes") around the screw dislocation line. If we pile up a set of such screw-dislocation-containing blocks vertically along the screw dislocation line, a cylindrical column of materials with screw dislocations would be formed, as illustrated in Figure 5c. We marked an equal-sized section in each of the blocks with a horizontal shift (s) between two neighboring layers, as shown in Figure 5a and b. If we now trace out the green sections in each of the successive blocks with a shift (s) between two adjacent blocks, we obtain the green strip in Figure 5c. Cutting out the green strip from the cylindrical structure in Figure 5c, we would arrive at a helical structure with periodicity (T), which resembles remarkably the observed SiC nanowires (Figure 5e). The strip can be divided into two zones, A and B (Figure 5d). In the A zone, the

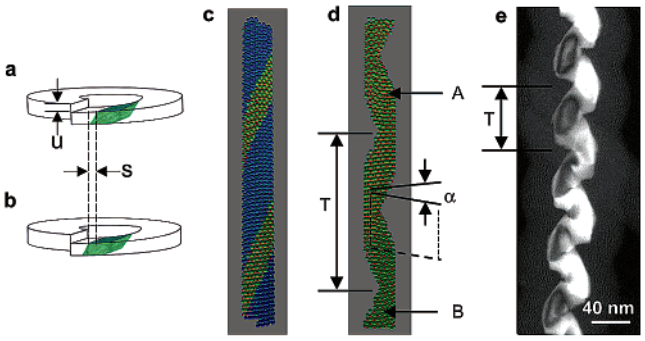

Figure 5. Schematic illustrations of the screw-dislocation-induced formation of helical SiC nanowires. (a), (b) Schematic drawings of two blocks each containing a screw dislocation with burgers vector, *u*, and helical ramps (helical lattice "planes") around the dislocation line. Green colored areas mark two equal-sized sections with a horizontal shift, *s*. (c) A cylindrical column with screw dislocations in the center, constructed by piling up a series of helical blocks shown in (a) and (b). The green strip is composed of the green sections shown in (a) and (b). (d) A helical structure cut out of the green strip of (c). *T* is the period of the helical structure, which has two different zones, A and B. α is the angle between the atomic layers in the two zones. (e) A dark field TEM image of a portion of the helical SiC nanowire. Note the resemblance between the TEM image and the model in (d).

atoms are in the back of the dislocation line; in the B zone, the atoms are in front of the dislocation line. The atomic layers in zones A and B are not parallel to each other, rather they have an angle (α) (Figure 5d). Although this angle was difficult to measure experimentally, Figure 5e shows a dark field TEM image, which exhibited different degrees of brightness for neighboring parts of the helical SiC nanowires, suggesting that the atomic layers in the neighboring parts are not parallel. This observation provides credence to the proposed screw-dislocation-induced growth mechanism for the helical SiC nanowires.

Our model suggests that the helical SiC nanowires constitute only parts of a column of screw dislocations, i.e., the strip marked in Figure 5c. This is most likely dictated by the initial nucleation sites, which might be too small to encompass a whole screw dislocation. The formation of the helical nanowires can be viewed as an epitaxy growth following the initial screw dislocation sites on the crystalline SiC nanoparticles. The simultaneous shift and rotation between successive layers are inherent characteristics of crystal screw dislocations and provide the driving force for the helical structure formation. The periodicities of the helical nanowires (Figure 5e), ranging from 40 to 80 nm are much larger than the Burgers vector of the dislocation, and they are determined primarily by the diameters of the SiC nanowires: thicker SiC nanowires tend to give larger periodicities for the helical nanostructures.

Screw dislocations are common in crystalline materials. The SiC helical nanowires may be a realization of the screw dislocations in SiC on a nanometer size scale. It should be possible to synthesize such helical nanowires for different crystalline materials under appropriate experimental conditions. Such helical nanowires may have wide ranges of applications in nanoelectronics, nanomechanics, reinforced composite materials, or nanosensors. Doped SiC/SiO_2 composite nanowires may allow novel device structures to be designed. For example, a high density of semiconductor-metal junctions can be manufactured by simply laying the helical nanowires on a flat metal surface.

Acknowledgment. This work was supported by NSF (DMR-0095828) and partly by the laboratory-directed research of Pacific Northwest National Laboratory. The work was performed at the EMSL, a national scientific user facility sponsored by DOE's Office of Biological and Environmental Research and located at Pacific Northwest National Laboratory, operated for DOE by Battelle. SEM characterizations by Drs. J. S. Young and J. Coleman and discussions with Drs. L. Li, F. Gao, T. Hubler, and D. McCready are gratefully acknowledged.

References

(1) Hu, J.; Odom T. W.; Lieber, C. M. *Acc. Chem. Res*. **1999**, *32*, 435.
(2) Dekker, C. *Phys. Today* **1999**, *52*, 22.
(3) Iijima, S. *Nature* **1991**, *354*, 56.
(4) Morales, A. M.; Lieber, C. M. *Science* **1998**, *279*, 208.
(5) Holmes, J. D.; Johnson, K. P.; Doty, R. C.; Korgel B. A. *Science* **2000**, *287*, 1471.
(6) Trentler, T. J.; Hickman, K. M.; Goel, S. C.; Viano, A. M.; Gibbons, P. C.; Buhro, W. E. *Science* **1995**, *270*, 1791.
(7) Gudiksen, M. S.; Lauhon, L. J.; Wang, J.; Smith, D. C.; Lieber, C. M. *Nature* **2002**, *415*, 617.
(8) Wu, Y. Y.; Fang, R.; Yang, P. D. *Nano Lett.* **2002**, *2*, 83.
(9) Björk, M. T.; Ohlsson, B. J.; Sass, T.; Persson, A. I.; Thelander, C.; Magnusson, M. H.; Deppert, K.; Wallenberg L. R.; Samuelson L. *Nano Lett.* **2002**, *2*, 87.
(10) Zhang, Y.; Suenaga, K.; Colliex, C.; Iijima, S. *Science* **1998**, *281*, 973.
(11) Pan, Z. W.; Dai, Z. R.; Wang, Z. L. *Science* **2001**, *291*, 1947.
(12) Zhang, H. F.; Dohnalkova, A. C.; Wang, C. M.; Young, J. S.; Buck, E. C.; Wang, L. S. *Nano Lett.* **2002**, *2*, 105.
(13) Rhodes, D.; Klug, A. *Nature* **1980**, *286*, 573.
(14) Weber, P. C.; Salemme, F. R. *Nature* **1980**, *287*, 82.
(15) Hirschberg, J. K.; Brunsveld, L.; Ramzi, A.; Vekemans J. M.; Sijbesma, R. P.; Meijer, E. W. *Nature* **2000**, *407*, 167.
(16) Berl, V.; Huc, I.; Khoury, R. G.; Krische, M. J.; Lehn, J. M. *Nature* **2000**, *407*, 720.
(17) Tang, Y. H.; Zhang, Y. F.; Wang, N.; Lee, C. S.; Han, X. D.; Bello, I.; Lee, S. T. *J. Appl. Phys*. **1999**, *85*, 7981.
(18) Mcllroy, D. N.; Zhang, D.; Kranov, Y.; Norton, M. G. *Appl. Phys. Lett*. **2001**, *79*, 1540.
(19) Kuzuya, C.; In-Hwang, W.; Hirako, S.; Hishikawa, Y.; Motojima, S. *Chem. Vap. Deposition* **2002**, *8*, 57.
(20) Iron powders: Alfa Aesar, purity 99.9%, size 200 mesh. Methane: Nor lab, purity 99%. Argon: Air Liquid America Corp., purity 99.99%.
(21) Zhang, B.; Wu, Y.; Yang, P.; Liu, J. *Adv. Mater*. **2002**, *14*, 122.
(22) Pan, Z. W.; Dai, Z. R.; Ma, C.; Wang, Z. L. *J. Am. Chem. Soc*. **2002**, *124*, 1817.
(23) Shi, W. S.; Zheng, Y. F.; Peng, H. Y.; Wang, N.; Lee, C. S.; Lee, S. T. *J. Am. Ceram. Soc*. **2000**, *832*, 3228.
(24) Wang, Z. L.; Dai, Z. R.; Gao, R. P.; Bai, Z. G.; Gole, J. L. *Appl. Phys. Lett*. **2000**, *77*, 3349.
(25) Amelinckx, S.; Zhang, X. B.; Bernaerts, D.; Zhang, X. F.; Ivanov, V.; Nagy, J. B. *Science* **1994**, *265*, 635.
(26) Suenaga, K.; Zhang, Y.; Iijima, S. *Appl. Phys. Lett*. **2000**, *76*, 1564.
(27) The nature of the carbon precursor is not known. Attempts to analyze the carbon precursor were not definitive. No carbon nanotubes or graphitic carbon were observed after the initial CH_4 flow, probably due to the high concentration of oxygen impurity in the initial reaction. However, large carbon fibers were observed after CH_4 reaction time longer than 15 min.
(28) Kittel, C. *Introduction to Solid State Physics*; Wiley: New York, 1986.
(29) During the review of this manuscript, another novel helical semiconductor nanowire of polycrystalline CdS was reported using supramolecular ribbon template by Sone, E. D.; Zubarev, E. R.; Stupp, S. I. in *Angew. Chem., Int. Ed*. **2002**, *41*, 1706.

NL025667T